AD-A094 062 MASSACHUSETTS INST OF TECH CAMBRIDGE DEPT OF MATERIA--ETC F/G 7/4
MOLECULAR-ORBITAL MODELS FOR THE CATAYLTIC ACTIVITY AND SELECTI--ETC(U)
DEC 80 A C BALAZS, K H JOHNSON N00014-75-C-0970
UNCLASSIFIED 12 NL

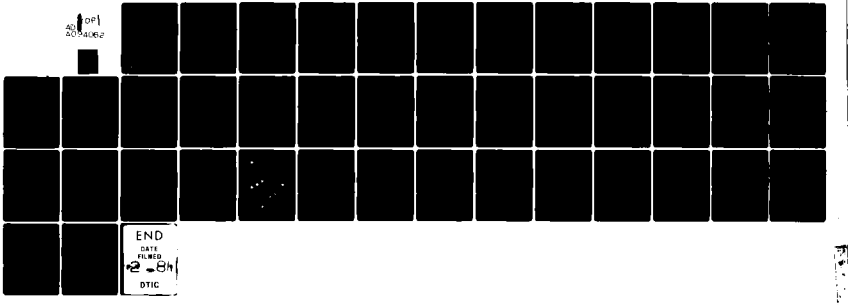

UNCLASSIFIED

SECURITY CLASSIFICATION OF THIS PAGE (When Data Entered)

REPORT DOCUMENTATION PAGE

READ INSTRUCTIONS BEFORE COMPLETING FORM

1. REPORT NUMBER	2. GOVT ACCESSION NO.	3. RECIPIENT'S CATALOG NUMBER
12	AD-A094 062	

4. TITLE (and Subtitle)

MOLECULAR-ORBITAL MODELS FOR THE CATALYTIC ACTIVITY AND SELECTIVITY OF COORDINATIVELY UNSATURATED PLATINUM SURFACES AND COMPLEXES.

5. TYPE OF REPORT & PERIOD COVERED

Interim

6. PERFORMING ORG. REPORT NUMBER

7. AUTHOR(s)

A. C. Balazs and K. H. Johnson

8. CONTRACT OR GRANT NUMBER(s)

N00014-75-C-0970

9. PERFORMING ORGANIZATION NAME AND ADDRESS

Department of Materials Science and Engineering
Massachusetts Institute of Technology
Cambridge, Massachusetts 02139

10. PROGRAM ELEMENT, PROJECT, TASK AREA & WORK UNIT NUMBERS

Task No. NR056-596

11. CONTROLLING OFFICE NAME AND ADDRESS

Office of Naval Research
Department of the Navy
Arlington, Virginia 22217

12. REPORT DATE

December 31, 1980

13. NUMBER OF PAGES

14. MONITORING AGENCY NAME & ADDRESS (if different from Controlling Office)

15. SECURITY CLASS. (of this report)

Unclassified

15a. DECLASSIFICATION/DOWNGRADING SCHEDULE

16. DISTRIBUTION STATEMENT (of this Report)

Approval for public release; distribution unlimited.

17. DISTRIBUTION STATEMENT (of the abstract entered in Block 20, if different from Report)

18. SUPPLEMENTARY NOTES

19. KEY WORDS (Continue on reverse side if necessary and identify by block number)

molecular-orbital models; catalytic activity; selectivity; coordinatively unsaturated; platinum surfaces and complexes.

20. ABSTRACT (Continue on reverse side if necessary and identify by block number)

Electronic structures have been calculated for 5-, 6-, and 10-atom Pt clusters, as well as for a $Pt(PH_3)_4$ coordination complex, using the self-consistent-field X-alpha scattered-wave (SCF-$X\alpha$-SW) molecular-orbital technique. The 10-atom cluster models the local geometry of a flat, unreconstructed Pt(100) surface, while the 5- and 6-atom clusters show features of a stepped Pt surface. $Pt(PH_3)_4$ resembles the chemically similar homogeneous catalyst $Pt(PPh_3)_4$. Common to all these coordinatively

DD FORM 1 JAN 73 1473 EDITION OF 1 NOV 65 IS OBSOLETE
S/N 0102-LF-014-6601

UNCLASSIFIED

SECURITY CLASSIFICATION OF THIS PAGE (When Data Entered)

unsaturated complexes are orbitals lying near or coinciding with the highest occupied molecular orbital ("Fermi level") which show pronounced d lobes pointing directly into the vacuum. Under the hypothesis that these molecular orbitals are mainly responsible for the chemical activities of the above species, one can account for the relative similarities and differences in catalytic activity and selectivity displayed by unreconstructed Pt(100) surfaces, stepped Pt surfaces or particles, and isolated $Pt(PPh_3)_4$ coordination complexes. The relevance of these findings to catalyst-support interactions is also discussed. Finally, relativistic corrections to the electronic structures are calculated and their implications on catalytic properties discussed.

MOLECULAR-ORBITAL MODELS FOR THE CATALYTIC ACTIVITY AND SELECTIVITY OF COORDINATIVELY UNSATURATED PLATINUM SURFACES AND COMPLEXES*

A. C. Balazs and K. H. Johnson

Department of Materials Science and Engineering

Massachusetts Institute of Technology

Cambridge, Massachusetts 02139

*Research sponsored by the Office of Naval Research and the National Science Foundation, Grant No. DMR-76-80895 (through the M.I.T. Center for Materials Science and Engineering.

Abstract

Electronic structures have been calculated for 5-, 6-, and 10-atom Pt clusters, as well as for a $Pt(PH_3)_4$ coordination complex, using the self-consistent-field X-alpha scattered-wave (SCF-Xα-SW) molecular-orbital technique. The 10-atom cluster models the local geometry of a flat, unreconstructed Pt(100) surface, while the 5- and 6-atom clusters show features of a stepped Pt surface. $Pt(PH_3)_4$ resembles the chemically similar homogeneous catalyst $Pt(PPh_3)_4$. Common to all these coordinatively unsaturated complexes are orbitals lying near or coinciding with the highest occupied molecular orbital ("Fermi level") which show pronounced d lobes pointing directly into the vacuum. Under the hypothesis that these molecular orbitals are mainly responsible for the chemical activities of the above species, one can account for the relative similarities and differences in catalytic activity and selectivity displayed by unreconstructed Pt(100) surfaces, stepped Pt surfaces or particles, and isolated $Pt(PPh_3)_4$ coordination complexes. The relevance of these findings to catalyst-support interactions is also discussed. Finally, relativistic corrections to the electronic structures are calculated and their implications on catalytic properties discussed.

Introduction

Much attention has been given to the characterization of the surface atoms constituting a catalytically active site [1]. Such sites can often be identified with low-coordination surface edges, corners, steps, and non-dense planes, and the observed catalytic activity may be attributed to unsaturated or "dangling" bonds at these locations. Identification and study of the "active sites" where chemical bond scission or rearrangement occurs, crucial to the working of a catalyst, ultimately requires that one investigate the electronic structure of the catalyst. For this problem, a cluster model, which treats the local interactions among a limited number of substrate atoms, is a logical theoretical approach. Numerous cluster molecular-orbital calculations have been carried out as a basis for investigating the chemisorptive and catalytic behavior of transition-metal aggregates and surfaces [2-5]. For Pt, theoretical studies have also included the application of the tight-binding band-structure approximation to various flat and stepped surface configurations, thereby producing the respective local density of states [6]. However, the tight-binding approximation is more appropriate for the 3d transition metals than the 5d series, which have a broader d band or more spatially delocalized d orbitals.

Using the self-consistent-field X-alpha scattered-wave (SCF-Xα-SW) molecular-orbital method [7,2], we have calculated the electronic structures of various clusters that model low-coordination Pt sites: a ten-atom cluster representing a non-dense "flat" surface, five- and six-atom clusters modeling step sites, and a $Pt(PH_3)_4$ coordination complex, which is chemically similar to the homogeneous catalyst $Pt(PPh_3)_4$. The strengths and weaknesses of the SCF-Xα-SW molecular-orbital method, along with the formalism and computational procedure, have been widely discussed in the literature [7].

Here, we point out two advantages of this techrique pertinent to the present problem: first, it permits accurate numerical evaluation of the molecular-orbital wavefunctions, thus allowing the real-space representation of surface states or "dangling bonds," and second, the calculations are carried out to full self consistency, thereby taking into account charge redistribution effects.

The Pt(100) surface reconstructs so that the atomic positions of the surface atoms do not lie in the equivalent bulk positions [8]. The reconstructed surface yields a (5 x 20) LEED pattern, suggesting a structure of hexagonal close-packed character. The unreconstructed surface can be prepared and gives by contrast a (1 x 1) LEED pattern. The electronic structure of the (1 x 1) surface, deduced from photoelectron emission measurements [8], includes a surface state or resonance 0.25 eV below the Fermi level which is not observed on the (5 x 20) surface. Moreover, the (1 x 1) surface dissociatively chemisorbs H_2 and O_2, whereas the (5 x 20) surface is inactive in this respect. Adsorption on the Pt(100)-(1 x 1) surface leads to strong attenuation in photoemission from this surface state/resonance peak. The above observations suggest that a surface state or "dangling bond" associated with this photoemission peak is participating strongly in bonding to adsorbates and may be responsible for the observed structure sensitivity for O_2 and H_2. In this paper, a ten-atom Pt cluster is arranged to simulate the local geometry of the unreconstructed Pt(100) surface (see Fig. 1). The objective is to identify features in the electronic structure of the cluster which can be related to the dissociative chemisorption properties described above.

The similarity in high chemisorptive and catalytic activity displayed

by the Pt(100)-(1 x 1) and Pt stepped surfaces [1] would make a comparison of their electronic structures instructive. Moreover, surfaces characterized by disorder such as steps and kinks provide good examples where a band-theoretical approach is inappropriate and cluster molecular-orbital calculations may be the more valid investigative technique. We report the results of calculations on two simple models for Pt stepped surfaces. Although these simple complexes do not resemble a particular stepped surface, they display geometric features common to all, such as edges and corners, as well as a lower coordination number compared to the "flat" site. While additional states due to surface steps in metals have not yet been definitively observed experimentally, one can attempt to describe the molecular orbitals that are precursors of these states. It should be emphasized that the catalytic properties of small transition-metal clusters [2,9] make the theoretical investigation of their electronic structures interesting in itself.

Finally, the activity of the coordinatively unsaturated homogeneous catalyst $Pt(PPh_3)_n$, n = 2, 3, 4, has frequently been compared to that displayed by a low-coordination chemisorption site on a Pt surface [10,11]. The catalytic activity of the n = 2 complex has already been investigated on the basis of SCF-$X\alpha$-SW molecular-orbital calculations [12]. In this paper, we describe the electronic structures of a $Pt(PH_3)_4$ complex and $Pt(Pt)_4$ cluster having the geometries shown in Fig. 2 and representing a low-coordination Pt site in the local environments of phosphine and platinum ligands, respectively, the latter cluster simulating the local environment on a stepped Pt surface. By comparing the respective electronic structures, it is hoped that a common molecular-orbital basis for understanding the activities of a homogeneous Pt catalyst and stepped Pt surface will be attained.

Pt(100) Surface

The cluster model used for the Pt(100) (1 x 1) surface is shown in Figure 1. The central surface atom is coordinated by all its first nearest neighbors and one second-nearest neighbor, the entire complex having C_{4v} symmetry. With a cluster of this configuration, one is able to characterize the molecular orbitals uniquely associated with the Pt(100) surface, which can then be correlated with observed surface activity. Clearly, we are most interested in orbitals that display charge localization on the central atom of the cluster, since it is this atom which has the greatest complement of nearest neighbors and hence a local environment most representative of a surface atom.

An outstanding feature of the Pt(100) (1 x 1) surface is the presence of a sharp peak in the ultraviolet photoelectron spectrum originating from an initial state just 0.25 eV below the Fermi level [8]. This peak has been attributed to the presence of a surface state or resonance which may be associated with an unsaturated "dangling bond" (sticking out perpendicular to the surface) and hence is expected to be active for chemisorption. The fact that dissociative chemisorption of various gases (H_2 and O_2) causes the intensity of this peak to diminish rapidly is consistent with these arguments.

The converged, spin-restricted SCF-Xα-SW molecular-orbital energy-level diagram for this cluster is shown in Figure 3. The highest occupied molecular orbital (HOMO) or "Fermi level," labeled $7b_2$, is slightly split off from the bulk of d orbitals. This orbital is predominantly d-like on all the metal centers, as in the bulk where the Fermi level runs through the top of the d band [2]. The orbital lies in the plane of the surface, with the majority of the charge localized on the central atom and the "top" neighbors (see Fig. 1). Examination of the wavefunction (Fig. 4) reveals

a net antibonding interaction between these centers, as would be expected of states at the top of the band [2,12]. Since this orbital has no lobes sticking out perpendicular to the surface, its potential for bonding with adsorbates is probably small. Hence, one can expect that this level will not play a major role in the chemisorptive and catalytic properties of the surface.

Further examination of the energy-level diagram in Fig. 3 reveals a small grouping of orbitals near the Fermi level. They lie above the block of predominantly nonbonding d orbitals, which display almost no charge on the central atom. Below this block lie the metal-metal bonding orbitals. Within the cluster of levels around the Fermi level (0.17 eV below it), lies an orbital labeled 12e, the wavefunction of which is shown in Fig. 5. (In the C_{4v} point group, the doubly degenerate e representation has basis functions that transform like d_{yz} and d_{xz} [13].) Again, the metal orbitals are d-like with significant charge localization on the central atom (see Table 1), which now however shows an antibonding interaction with its neighbors in the yz plane, perpendicular to the plane of the surface. On the central atom, the lobes of the d_{yz} orbital component can be clearly seen to point away from the surface, extending into the vacuum. These lobes could facilitate dissociative chemisorption of H_2 or O_2 by donating charge into the symmetry-compatible antibonding σ_u or π^* orbitals, respectively, of these molecules [12]. Helms et al. [8] speculate that the loss of intensity from the photoemission peak associated with the surface state suggests charge transfer taking place from the Pt surface to the dissociatively chemisorbed H_2 or O_2.

Lying just below the 12e orbital is the 11e orbital which also displays the characteristics cited above (see Fig. 5). Again, the d_{yz} orbital

component localized on the central atom is spatially pointed away from the surface in the direction of the vacuum.

Lying directly below the 11e level and 0.44 eV below the Fermi level is the $9a_1$ orbital, shown in Fig. 5, which has d_{z^2} character on the central atom pointing perpendicularly out of the surface. This orbital is capable of participating in σ-bonding with symmetry-conserving orbitals of impinging reactants. Previous extended-Hückel-type Ni cluster calculations have indicated the d_{z^2} orbital to be most important for chemisorption on the surface [3]. However, the presence of both $d_{yz}(d_{xz})$ and d_{z^2} types of orbitals near the Fermi energy, with their lobes pointing out into the vacuum, indicated by the present SCF-Xα-SW cluster model, suggests that this surface can trap diatomic molecules (for example) striking the surface with a variety of orientations. If a diatomic molecule is colinear with a surface atom and perpendicular to the surface, it will mix its π and π^* orbitals with the metal d_{yz} and d_{xz} orbitals, and where z is the colinear direction, it will mix its σ_{pz} and σ^*_{pz} orbitals with the metal d_{z^2} orbital [5]. The presence of these orbitals also suggests that the initial dissociative step in the chemisorption of small molecules such as H_2 on a Pt surface should be more favorable over an atomic site [12] than at a surface interstitial site. Thus the 12e, 11e, and $9a_1$ orbitals may be viewed as collectively constituting the "dangling bonds" that are primarily responsible for the observed activity of the Pt(100) (1 x 1) surface. The general location of these levels with respect to the highest occupied molecular orbital, $7b_2$, in Fig. 3 is consistent with the photoemission peak suggesting a surface state or "resonance" $\sim$ 0.25 eV below the Fermi energy [8]. However, angle-resolved photoemission measurements are necessary to resolve the individual contributions of these orbitals.

Since the availability of lobes of polarizable charge is important in the initial stages of chemisorption, it is essential to examine the charge distribution in the cluster (Fig. 1) representing the Pt(100) (1 x 1) surface. Those atoms of the cluster coincident with the (100) surface plane are somewhat positively charged with respect to the underlying atoms representing the "bulk," consistent with the findings of previous SCF-Xα-SW calculations for 13-atom Pt, Pd, and Ni clusters [2]. In Ref. [2] the migration of electronic charge from "surface" to "bulk" was explained as due, at least in part, to the fact that the potentials of coordinatively unsaturated atoms at the surface are less attractive than those of the fully coordinated interior bulk atoms. Other electronic-structure calculations for Ni clusters [3-5] have indicated a flow of charge in the opposite direction, i.e., toward the surface atoms. However, these calculations were either of the non-self-consistent Xα-SW type (Ref. [4]) or of the non-iterative extended-Hückel type (Refs. [3] and [5]). Neither of these latter procedures adequately allow for charge redistribution, and it was shown in Ref. [2] that a change in extended-Hückel calculational parameters can give quite different charge distributions.

Most notably, the present SCF-Xα-SW results do indeed indicate a variation in the charge distribution around the surface layer that is confirmed experimentally, for example by the differences in value for the bulk and surface part of the work function [14]. Specifically, this variation in charge gives rise to surface dipole moments which in turn affect the work function of the surface. It is known that the work functions of closely packed surfaces are larger than those for loosely packed and stepped surfaces [1,14]. The lower work function for loosely packed and stepped surfaces makes charge transfer from the metal to the reactants more facile. This may also account for the greater activity of these surfaces and lends credence to our model of charge transfer from the filled metal $d_{yz}(d_{xz})$ orbitals to empty σ_u or π^* levels as

an important factor in surface reactivity [12].

A close-packed vs. open structure also makes a difference when considering the concept of "dangling bonds" at the surface. On fcc metals, the more open a structure, the more bonds that are severed in creating the surface and consequently the more dangling bonds that are created [8]. It becomes attractive to associate high chemisorption activity with low-coordination Pt surface atoms, whether they be in steps or the less closely packed surfaces such as Pt(100) (1 x 1). Conversely, since the Pt(100) (5 x 20) surface is hcp-like in structure, with fewer dangling bonds exposed to the vacuum, one can understand how its activity would be diminished.

Furthermore, when the calculated local density of states (LDS) for a non-dense surface is decomposed into its orbital components, it is the d_{xy}-type orbitals (those lying within the surface plane) that more nearly approximate the LDS of a bulk atom, whereas the d_{yz}-, d_{xz}-, and d_{z^2}-type orbitals (those pointing perpendicularly outward from the surface) are responsible for the "surface states" and "dangling bonds" discussed above [6,15]. Consequently, this evidence would further pinpoint the source of high chemisorptive activity to the d_{yz}, d_{xz}, and d_{z^2} orbitals on these low-coordination surfaces. These observations fully coincide with our findings.

Finally, it is interesting to note that the antibonding interactions between the central atom and the "surface" atoms are primarily localized in the xy plane. It appears that it is antibonding interactions with the underlying "bulk" atoms that produce lobes on the central atom that point away from the surface and into the vacuum.

Stepped Pt Surfaces

The importance of structural defects such as steps and kinks for catalytic bond breaking on metal surfaces has been emphasized in recent years [1]. A

variety of experiments have attested to increased rates of reactions and sticking coefficients on Pt steps in particular. This behavior raises the question of which specific physical properties associated with step edges give rise to the observed enhancement. The theoretical description and calculation of adsorption kinetics at present are not even tractable for well characterized low index surfaces, one must therefore consider more qualitative arguments for rationalizing step-enhanced adsorption kinetics. We will investigate the hypothesis that these special properties of steps are due to the presence of "dangling" or coordinatively unsaturated bonds centered on the edge atoms. Hence, we will again be looking for high-lying molecular orbitals that could contribute to the observed phenomena. The cluster models (I and II in Fig. 2) we have chosen allow one to isolate the bonding interactions not only at corner but also along edge locations on a simple Pt step.

Model II (Fig. 2) is the more appropriate cluster for discussing edge-edge interactions since both "edge" atoms (those along the plus and minus y axis) see the same "bulk" environment. However, investigation of both clusters leads to remarkably similar results. Consequently, our discussion will revolve around results for Model I, using orbitals from Model II to supplement these observations on the former cluster. The atoms located in the lower half of the yz plane will be considered as the "bulk" atoms, corresponding to the atoms located in the terrace plane and at the bottom of the step. The atoms along the positive and negative directions of the x-axis are edge neighbors of the central atom, located at the origin. The Pt-Pt nearest-neighbor distance was used as the length between each metal center and the one at the origin.

The SCF-$X\alpha$-SW energy-level diagram for the 5-atom cluster of Model I is shown in Figure 6. The smaller d band width (as compared with experiment and the d band width of the previous 10-atom cluster) is due to the reduced

cluster size. Nevertheless, the electronic structure is similar to that of larger Pt clusters, since a manifold of antibonding orbitals are split off from a block of nonbonding d orbitals (exhibiting no charge on the central atom), with the metal-metal bonding orbitals split off the bottom of this nonbonding band. Clustered around the HOMO, $6b_2$, are the $8a_1$, $5a_2$, $6b_1$, and $7a_1$ orbitals. The $9a_1$ orbital is the LUMO. Some of these orbitals are shown in Figure 7 (also see Table 2). One can see not only the antibonding interactions between the central atom and bulk atoms but also between the edge atoms. Similar interactions can be seen among the high-lying orbitals of Model II, for example, in the $8b_2$ HOMO as well as the high-lying $7b_2$ and $7b_1$ orbitals (see Figure 8). Characteristic of all these orbitals are lobes that stick out into the vacuum, pointing away from the surface. In fact, it can be said that the LDS, around the Fermi level, is dominated by orbitals that display this feature. Perhaps most notable among the results of Model I are the $6b_2$ and $7a_1$ orbitals shown in Fig. 7. The d_{yz} and d_{z2} orbitals on the central atom in these respective orbitals protrude most prominently while pointing perpendicularly away from the open face of the step. Here, as in the previous example of the unreconstructed Pt(100) surface, the $6b_2$ d_{yz} orbital can donate charge into an unoccupied σ_u or π^* orbital of a reactant, while the $7a_1$ d_{z2} orbital can participate in σ-type bonding to an adsorbate, as can the LUMO $9a_1$. In Model II, we find that two neighboring edge sites can also initiate such bonding interactions. Examination of the $8b_2$ HOMO in Fig. 8 shows two adjacent antibonding d_{z2} orbitals. Taken together, these "out-of-phase" d-orbitals are capable of charge transfer from the metal to σ_u or π^* reactant orbitals. In fact, it may be the "dangling-bond" character of the above orbitals that is so effective in trapping gas-phase reactants. This hypothesis is strongly supported by the recent experimental work of Gale et al. [16], who discovered that the reaction for H_2-D_2 exchange depends on the reactant

angle of incidence. An enhanced reaction probability is observed if the reactant beam strikes the open side of the step structure. The authors [16] speculated that this is the direction in which available bonding orbitals of the surface atoms are pointing.

This explanation was also proposed by Christmann and Ertl [17], who observed that a step density of 11% of the surface atoms increases the initial sticking coefficient by a factor of four and the activity for the H_2-D_2 exchange reaction by an order of magnitude (with the apparent activation energy for H-H bond breaking remaining constant). These authors [17] also conclude that these phenomena can be explained by the enhanced activity of the metal atoms at the stepped site to trap impinging reactants. Their schematic model for the adsorption of hydrogen atoms at a step is entirely consistent with H_2 being dissociatively chemisorbed through interaction with the occupied d_{yz} orbital of the metal atom located at the step edge.

Further support for this interpretation is given by observed changes in the work function [17]: adsorption of hydrogen at step sites increases the work function, whereas adsorption on the Pt(111) plane leads to a monotonic decrease of the work function. The increase in work function implies that the hydrogens carry a small excess negative charge, thereby supporting the possibility of charge transfer from the metal step to the adsorbed species. In fact, a slightly higher (by 2.3%) binding energy for the step site was observed [17].

While many of the reported investigations on stepped Pt surfaces deal with H_2 bond breaking, step sites have also been found to have a strong influence on the dissociative chemisorption of O_2 as well. Thermal desorption spectroscopic studies performed by Collins and Spicer [18] yielded estimates for the saturation O coverage for various Pt surfaces. The latter values suggest that

dissociative chemisorption of O_2 takes place primarily at step or defect sites. The partially occupied π^* orbitals of O_2 are symmetry-compatible with the occupied metal d_{yz} orbital of the Pt_5 $6b_2$ HOMO in Fig. 7, for example, and thus forward donation from this orbital may play a significant role here as well as in the example of dissociative H_2 chemisorption.

In the previous section, it was noted that a decrease in the work function accompanies a decrease in the packing density of metal faces. Similarly, there exists a lowering of the work function as the step density is increased [1], which may indicate the existence of a net positive charge at edge atoms. This finding can qualitatively be explained in terms of a smoothing effect of the electronic charge density which does not follow sharp edges as exhibited by step atoms. Again a slight positive charge exists at the corner and edge atoms in the chosen cluster models (Fig. 2), consistent with earlier results of SCF-Xα-SW calculations for 13-atom Pt clusters [2]. These polarized lobes may induce polarization of the incoming molecules and could influence their orientation, thereby causing an enhancement of the sticking coefficient [17].

Finally, it should be emphasized that the variety of reactive orbitals centered on the edge atoms (all symmetries of the C_{2v} point group are represented in the manifold of orbitals around the HOMO) increases the diversity of bonding possibilities. Previous SCF-Xα-SW calculations for Ni, Pd, and Pt clusters [2] also suggest a diversity of "dangling-bond" orbitals at a "step" site. This difference in local electronic structure at flat and stepped surface sites is most likely a key factor in the enhanced catalytic activity of steps. For the unreconstructed Pt(100) surface, only the $d_{yz}(d_{xz})$ and d_{z^2} orbitals have lobes pointing directly into the vacuum, whereas, for the stepped surface, not only the orbitals cited above but

also the d_{xy} and $d_{x^2-y^2}$ components (for example, the $5a_2$ and $9a_1$ orbitals, respectively, in Fig. 7) display the desired directionality.

$Pt(PH_3)_4$

In this section we examine the possible relationships between the homogeneous catalytic activity of coordinatively unsaturated platinum complexes and the heterogeneous activity of low-coordination (e.g., "step") sites on platinum surfaces. Reactions involving the Pt(0)-triphenylphosphine complexes $Pt(PPh_3)_n$, where n = 2, 3, 4, have been shown to have precise analogues on Pt surfaces [11]. As a basis for understanding these correspondences, we compare the electronic structures of $Pt(L)_n$ clusters which, for the ligands $L = PH_3$, represent the above coordination complexes and for L = Pt, represent the local environment of a low-coordination Pt surface site. We have already reported preliminary results of such a comparison for the case n = 2 [12].

We consider now the n = 4 case, in which the four Pt atoms surrounding the central Pt site in Model I [Fig. 2] for a Pt step site are replaced by phosphine ligands, producing the $Pt(PH_3)_4$ molecule. As in previous calculations [12], the triphenylphosphine (PPh_3) group is modeled by the simpler but chemically similar phosphine (PH_3) group. The appropriate Pt-P bond distances have also been substituted, but the geometry of the 5-atom Pt cluster of Model I has been preserved. In this way, one can observe the similarities and differences between the electronic structures of the central Pt atom in the respective phosphine and metal local environments, while conserving orbital symmetries. This should allow one to develop a common molecular-orbital basis for understanding homogeneous and heterogeneous catalytic properties.

At first glance, the energy level diagram for $Pt(PH_3)_4$ shown in Fig. 9 reveals a rather different electronic structure from that displayed by the

metal cluster (cf. Fig. 6), although here, too, platinum-ligand (Pt-L*) antibonding orbitals are split off in energy from the top of a group of nonbonding orbitals, while the Pt-L bonding orbitals are split off from the bottom. The nonbonding d orbitals (n.b.d.) here are nonbonding with respect to the phosphine ligands, with essentially all the charge localized on the metal center. However, the highest occupied antibonding orbitals, $8a_1$ and $5b_2$, responsible for the catalytic activity of the $Pt(PH_3)_4$ complex, lie higher in energy than the corresponding orbitals, $8a_1$ and $6b_2$, of the Pt_5 cluster (cf. Figs. 9 and 6). This situation may reflect the lower electronegativity of the Pt-P* orbitals arising from the greater donating power of the phosphine ligands in the molecule. In fact, in the $Pt(PH_3)_4$ molecule, the Pt atom has a small net effective negative charge. Compared with this metal atom, the surface atoms represented by the Pt_5 and Pt_{10} clusters are electron deficient and hence less nucleophilic [11]. One would then expect the $Pt(PPh_3)_4$ complex to be a stronger electron donor than the surface species. This observation is substantiated by the fact that unsaturated hydrocarbons act as net electron donors to platinum surfaces, whereas in such zerovalent platinum complexes as $Pt(PPh_3)_2(C_2H_4)$ and $Pt(PPh_3)_2(C_2H_2)$, the alkenes and alkynes are net electron acceptors. Indeed, it may be noted that the lowest unoccupied molecular orbital of the Pt_5 cluster is of a_1 symmetry (see Fig. 6), the symmetry that is compatible with forward donation from a high-lying σ reactant level. For the $Pt(PH_3)_4$ complex, the LUMO transforms like the b_2 representation (Fig. 9), which is not symmetry compatible with this type of forward donation.

The manifold of Pt-L levels is broader than the width of the Pt_5 cluster d band (cf. Figs. 9 and 6), indicating that the bonding-antibonding interactions exerted by the phosphine ligands on the central Pt atom are

greater than those exerted by the neighboring metal atoms of the cluster. This is as would be expected for interacting species which do not share identical electronegativities. Whereas there exists a clustering of orbitals around the Fermi level in the Pt_5 cluster, the corresponding levels in the $Pt(PH_3)_4$ complex extend from the $8a_1$ HOMO to the antibonding $5b_2$ orbital (located 1.2 eV below $8a_1$) to the three nonbonding d levels (lying 4 eV below $8a_1$). Since the $Pt(PH_3)_4$ nonbonding d orbitals are considerably suppressed in energy, they will be less reactive than those clustered around the Fermi level in the all-Pt complex. As previously discussed, this clustering of the Pt_5 antibonding d orbitals allows, in principle, the complex to participate in or catalyze a wide variety of reactions, since every orbital symmetry of the C_{2v} point group is represented near the Fermi level. However, only those reactants that have high-lying levels which are symmetry compatible with the a_1 or b_2 symmetries can readily interact with the $Pt(PH_3)_4$ complex, making the latter more selective in the types of reactions it can catalyze. It is these ligand effects that seem to account for the higher selectivity frequently observed for homogeneous catalysts. It should be noted that a $Pt(PH_3)_4$ complex can accommodate a wide variety of reactants only through its ability to eliminate one or two phosphine ligands [11] and thereby expose metal d levels of differing energies and symmetries.

Recent experimental work suggests that the interactions between catalytic metal particles and their supporting environments (typically refractory oxides) are of sufficient magnitude as to suggest significant chemical and electronic modifications of the metal at the metal-support interface [19,20]. These findings are confirmed by recent SCF-Xα-SW molecular-orbital studies of supported metal catalysts. For example, SCF-Xα-SW calculations have been carried out for "raft-like" configurations of Pt and Ru atoms on silica

(SiO_2) [21]. The primarily covalent interaction between the metal d orbitals and oxygen nonbonding 2p orbitals that constitute the top portion of the SiO_2 valence band lead to metal-oxygen bonding orbitals embedded in the valence band and to nonbonding and antibonding d orbitals split off in energy from the top of the valence band and positioned within the SiO_2 band gap like "deep-level" transition-metal impurity states in the band gap of a semiconductor. The highest of these antibonding orbitals is principally metal d_{yz} in character for the chosen coordinate system and has a one-to-one correspondence with the HOMO of a coordinatively unsaturated $(PH_3)_2$ Pt complex [12]. The orbital symmetries and orderings are qualitatively similar for SiO_2Pt and SiO_2Ru, although in the latter system, the d_{yz} antibonding orbital is empty. This difference in orbital occupancy suggests that the bonding and catalytic activity of Ru atoms on silica should be significantly different from those of Pt atoms on silica. Recent EXAFS, electron microscopy, and chemisorption studies [19] indicate that ruthenium interacts strongly with a silica substrate, forms "raft-like" structures, and chemisorbs oxygen (O_2) molecularly, whereas these properties have not yet been demonstrated for silica-supported platinum. SCF-Xα-SW cluster models for ruthenium aggregates on SiO_2 suggest that the SiO_2-Ru bonding perpendicular to the silica surface actually enhances Ru-Ru bonding parallel to the surface, thereby providing a theoretical justification for the formation of raft-like structures [21]. SCF-Xα-SW molecular-orbital studies of strong metal-support interactions between platinum and titanium dioxide (TiO_2) have also recently been reported [22], with the results in good agreement with experiments.

Thus, one may be able to attribute the greater selectivity displayed by certain supported metal catalysts to the type of effects found in the above

studies. The chemical bonding-antibonding interaction between the supporting environment and metal atoms at the interface can remove the degeneracy or near degeneracy of the metal d orbitals and thereby alter the activity of these metal sites from that characteristic of the elemental metal environment. Clearly, these effects will depend on the degree of metal dispersion and will be most significant in the limit of low dispersion, e.g., rafts vs. particles.

Yet, despite these important factors, notable similarities exist among active metal (e.g., Pt) surfaces of different morphologies. As described earlier in this paper, the most reactive orbitals in both the Pt(100) (1 x 1) and Pt stepped surfaces are those which lie perpendicular to the plane of the surface or on the open side of the step, respectively. In our chosen coordinate system these are the d_{z^2} and d_{yz} (d_{xz}) orbitals (see Figs. 5, 7, and 8). It is precisely these orbitals that stand out as the reactive antibonding levels in the $Pt(PH_3)_4$ system as well (see Fig. 10). The $Pt(PH_3)_4$ $8a_1$ d_{z^2} orbital has more s and p character than the d_{z^2} levels of the metal clusters (see Table 1) and the $5b_2$ orbital shows some overlap between the upper lobes of the d_{yz} orbital and the phosphorus p orbital not found in the antibonding interactions between neighboring metal d orbitals. However, the similarities in orbital structure outweigh the differences and may account, at least in part, for the similar reactivities displayed by low-coordination Pt surface sites and coordinatively unsaturated $Pt(PPh_3)_n$ complexes.

Relativistic Effects

Since special relativistic effects can, in principle, influence the electronic structure, and therefore the chemistry, of heavy-metal clusters and complexes [23], relativistic corrections to the Pt_{10} and $Pt(PH_3)_4$ electronic structures considered in the preceding sections of this paper have been

calculated, using a recently developed relativistic version [24] of the SCF-Xα-SW method which determines relativistic molecular-orbital energy-level shifts (neglecting spin-orbit level splittings). For the 10-atom Pt cluster representing the Pt(100) (1 x 1) surface, the main effect of relativity is to widen the d band, an effect that has been observed in previous relativistic SCF-Xα-SW calculations for Pt_4 and Pt_4H clusters [23]. The fully self-consistent relativistic electronic structure of the Pt_{10} cluster is shown in Fig. 11 and may be compared with the nonrelativistic results shown in Fig. 3. Although this general widening of the d band occurs, the 11e, 12e, and $9a_1$ orbitals of Fig. 3, described earlier as the Pt(100) (1 x 1) surface reactive "dangling-bond" orbitals, still lie within $\sim$ 0.4 eV below the Fermi level. However, these levels are labeled 12e, 13e, and $7a_1$, respectively, in Fig. 11 because of relativistic changes in level orderings within the d band. Furthermore, the charge distributions and hybridizations of these "dangling-bond" orbitals are largely unaltered by the relativistic effects (cf. Tables 1A and 1B).

For the $Pt(PH_3)_4$ complex, the nonbonding d orbitals ($7a_1$, $3a_2$, $5b_1$) and the highest occupied antibonding d orbital ($5b_2$) are shifted uniformly upward in energy by the relativistic effects (cf. Figs. 9 and 12), reflecting the general tendencies of d orbitals under relativistic corrections. Since s and p orbitals generally experience a "downward" shift in energy due to relativity, the highest occupied orbital ($8a_1$) of $Pt(PH_3)_4$, which has a small admixture of s and p character along with its predominant d character, shows a smaller net shift upward in energy when relativistic effects are included (cf. Figs. 9 and 12). Consequently, the energy gap between the $5b_2$ and $8a_1$ orbitals decreases to 0.9 eV (Fig. 12) from the nonrelativistic value of 1.2 eV (Fig. 9). In Table 1, it is again evident

that the relativistic charge distributions and hybridizations of the orbitals responsible for the reactivity and homogeneous catalytic activity of the $Pt(PH_3)_4$ complex are very similar to those calculated in the nonrelativistic limit.

It would appear, on the basis of these calculations, that the effects of special relativity do not significantly alter our conclusions about the reactivities and catalytic activities of Pt complexes and surfaces, including stepped surface sites, since the directionalities and relative energies of the high-lying "dangling-bond" orbitals are essentially unperturbed. Nevertheless, spin-orbit splittings of these orbitals, which have not been calculated in the present work, can be of some importance [25], and the upward shifts in energy of the highest occupied orbitals lowers their orbital electronegativities [26] and thus, in principle, makes them better electron donors.

Summary and Conclusions

It has been found through first-principles SCF-$X\alpha$-SW molecular-orbital calculations that the local electronic structures of a Pt(100) (1 x 1) surface, a Pt surface "step" site, and a coordinatively unsaturated $Pt(PH_3)_4$ complex are remarkably similar. Common to all these systems is the presence of unsaturated or "dangling" Pt d orbitals which, through "metal-ligand" antibonding interactions with near-neighbor atoms, are raised in energy to be near or coincide with the highest occupied molecular orbital ("Fermi level") of the system. From the SCF-$X\alpha$-SW molecular-orbital wavefunctions, it can be seen that the Pt d lobes of these orbitals are spatially directed away from their neighbors into the vacuum. Consequently, they are free to interact with symmetry-conserving orbitals of impinging gas-phase reactants. Under the hypothesis that these "dangling-bond" orbitals are responsible for the catalytic activities of the above systems, one can account for a number of

experimental observations.

For example, on a stepped Pt surface or particle, we have found a diversity of reactive d orbitals near the Fermi energy carrying a small effective positive charge and pointing out from the edge sites on the open side of the step. The presence of these orbitals correlates well with the relatively high catalytic activity displayed by Pt step sites.

The similarity in orbital character for a $Pt(PH_3)_4$ complex and that of an elemental Pt cluster having the same geometry may explain the parallel activities of low-coordination Pt surface sites and homogeneous Pt catalysts. However, the greater selectivity exhibited by most homogeneous Pt catalysts may be accounted for by the interactions of the metal d orbitals with the "lone-pair" p orbitals of the nonmetallic (e.g., PH_3) ligands.

Detailed SCF-X_α-SW molecular-orbital models for the reductive elimination ("reforming") of H-H, H-CH_3, and CH_3-CH_3 bonds by homogeneous Pt, Pd, and Ni catalysts will appear as a separate publication [27].

References

[1] For example, see the review article by H. Wagner, in Springer Tracts in Modern Physics, Vol. 85, ed. G. Höhler (Springer-Verlag, Berlin, 1979) p. 151.

[2] R. P. Messmer, S. K. Knudson, K. H. Johnson, J. B. Diamond, and C. Y. Yang, Phys. Rev. B13 (1976) 1396.

[3] D. J. M. Fassaert, H. Verbeek, and A. Van der Avoird, Surface Sci. 29 (1972) 501.

[4] P. L. Jennings, G. S. Painter, and R. O. Jones, Surface Sci. 60 (1976) 255; R. O. Jones, P. J. Jennings, and G. S. Painter, Surface Sci. 53 (1975) 409.

[5] A. B. Anderson and R. Hoffmann, J. Chem. Phys. 61 (1974) 4545.

[6] M. C. Desjonquires and F. Cyrot-Lackmann, Solid State Comm. 18 (1976) 1127.

[7] J. C. Slater and K. H. Johnson, Phys. Rev. B5 (1972) 844; K. H. Johnson in Advances in Quantum Chemistry, Vol. 7, ed. P.-O Löwdin (Academic Press, New York, 1973) p. 143; J. C. Slater, The Self Consistent Field for Molecules and Solids, Vol. 4 of Quantum Theory of Molecules and Solids (McGraw-Hill, New York, 1974) p. 101; K. H. Johnson in Annual Review of Physical Chemistry, Vol. 26, eds. H. Eyring, C. J. Christensen, and H. S. Johnston (Annual Reviews, Palo Alto, 1975) p. 39.

[8] C. R. Helms, H. P. Bonzel, and S. Kelemen, J. Chem. Phys. 65 (1976) 1773.

[9] R. Van Hardeveld and F. Hartog, Adv. Catal. 22 (1972) 75.

[10] R. Ugo, G. LaMonica, F. Cariati, S. Cenini, and F. Conti, Inorg. Chim. Acta 4 (1970) 390.

[11] T. A. Clarke, C. C. Gay, and R. Mason, in The Physical Basis for Heterogeneous Catalysis, ed. E. Drauglis and R. I. Jaffee (Plenum Press, New York, 1975).

[12] K. H. Johnson, A. C. Balazs, M. Kolari, Surface Sci. 72 (1978) 733.

[13] F. A. Cotton, Chemical Applications of Group Theory (Wiley-Interscience, New York, 1971) p. 357.

[14] J. Hölzl and F. K. Schulte, Springer Tracts in Modern Physics, Vol. 85, ed. G. Höhler (Springer-Verlag, Berlin, 1979) p. 1.

[15] J. R. Schrieffer and P. Soven, Phys. Today 28 (1975) 24.

[16] R. J. Gale, M. Salmeron, and G. A. Somorjai, Phys. Rev. Letts. 38 (1977) 1027.

[17] K. Christmann and G. Ertl, Surface Sci. 60 (1976) 365.

[18] D. M. Collins and W. E. Spicer, Surface Sci. 69 (1977) 85.

[19] R. J. Lisle, G. H. Via, and J. H. Sinfelt, J. Chem. Phys. 67 (1977) 3831.

[20] J. Anderson, Structure of Metallic Catalysts (Academic Press, New York, 1975) p. 276.

[21] K. H. Johnson and M. J. Kolari (to be published).

[22] J. A. Horsley, J. Am. Chem. Soc. 101 (1979) 2870.

[23] R. P. Messmer, D. R. Salahub, K. H. Johnson, and C. Y. Yang, Chem. Phys. Letts. 51 (1977) 84.

[24] The relativistic corrections were developed and programmed by J. H. Wood and A. M. Boring. The theoretical basis for this is given in J. H. Wood and A. M. Boring, Phys. Rev. B18 (1978) 2701.

[25] D. Case (private communication); D. Case and C. Yang (to be published).

[26] K. H. Johnson, J. Vac. Sci. Technol. 15 (1978) 410.

[27] A. C. Balazs, K. H. Johnson, and G. M. Whitesides, J. Am. Chem. Soc. (submitted for publication).

TABLE I

Charge distributions and partial wave decomposition for the central Pt atom in the "dangling bond" orbitals for the Pt_{10} and $Pt(PH_3)_4$ clusters. Section A presents these values without relativistic corrections while the values in Section B include the corrections.

Section A

Pt_{10}

Level	Orbital Energy (eV)	Percent Charge	Partial-Wave Character s	p	d
12e	-5.5469	12.12		0.95	99.05
11e	-5.8070	10.04		4.03	95.97
$9a_1$	-5.8119	22.46	2.78	2.45	94.77
		$Pt(PH_3)_4$			
$8a_1$	-3.2775	37.30	7.85	16.98	75.17
$5b_2$	-4.5339	62.49		13.04	86.96

Section B

Pt_{10}

13e	-5.2378	11.50		3.21	96.79
12e	-5.3234	8.15			100.00
$7a_1$	-5.6388	24.71	3.33	3.78	92.89
		$Pt(PH_3)_4$			
$8a_1$	-3.1698	32.02	13.11	21.87	65.02
$5b_2$	-4.0942	70.68		12.79	87.21

TABLE 2

Charge distributions and partial-wave decomposition for the central metal atom in the "dangling bond" orbitals for tne Pt_5 cluster.

Pt_5

Level	Orbital Energy (eV)	Percent Charge	Percent Partial-Wave Character		
			s	p	d
$9a_1$(LUMO)	-5.1895	22.35	2.85	0.62	96.5
$6b_2$(HOMO)	-5.3417	22.07		2.85	97.1
$5a_2$	-5.5817	28.7			100.00
$6b_1$	-5.6317	30.48		0.42	99.58
7a	-5.6725	23.46	0.07	0.66	99.27

Charge distributions and partial-wave decomposition for the "edge" atoms (along the plus and minus x-axes) in the "dangling bond" orbitals for the Pt_5 cluster.

Level	Orbital Energy (eV)	Percent Charge (Combined)	Percent Partial-Wave Character		
			s	p	d
$9a_1$(LUMO)	-5.1895	12.51	4.27	2.25	93.47
$6b_2$(HOMO)	-5.3417	2.29		0.30	99.70
$5a_2$	-5.5817	36.14		0.56	99.44
$6b_1$	-5.6317	52.63	1.04	0.65	98.32
$7a_1$	-5.6725	4.38	5.82	1.69	92.50

Figure Captions

Figure 1. Ten-atom cluster representation of the local geometry of the unreconstructed Pt(100) surface.

Figure 2. Five (Model I) and six (Model II) atom cluster representations of a Pt stepped surface.

Figure 3. SCF-Xα-SW molecular-orbital energy levels for the Pt_{10} cluster. Levels are labeled according to the irreducible representations of the C_{4v} symmetry group. Highest occupied level is indicated by an arrow. The closely spaced nonbonding d levels (n.b.d) are hatched in.

Figure 4. Contour map for the $7b_2$ HOMO of the Pt_{10} cluster. The contour values are 0.003, 0.009, 0.027, and 0.081. The d_{xy} component is localized on each metal center, the entire orbital lying in the *xy plane (parallel to the plane of the surface).*

Figure 5. The d_{yz} and d_{z^2} components of the Pt_{10} 12e, 11e, and $9a_1$ orbitals, respectively. The orbitals lie in the *yz* plane.

Figure 6. SCF-Xα-SW molecular-orbital energy levels for the Pt_5 cluster (Model I). Levels are labeled according to the irreducible representations of the C_{2v} symmetry group. Highest occupied level is indicated by an arrow.

Figure 7. Contour maps of the high lying $6b_2$ (d_{yz}, HOMO) $5a_2$ (d_{xy}), $6b_1$(d_{xz}), $7a_1$ (d_{z^2}), and $9a_1$ ($d_{x^2-y^2}$, d_{z^2}, LUMO) orbitals of the Pt_5 stepped surface. Note that in the C_{2v} point group, the a_1 irreducible representation transforms like the d_{z^2} and $d_{x^2-y^2}$ basis functions.

Figure 8. Contour maps for the high lying $8b_2$ (d_{z^2}, HOMO), $7b_2$ (d_{yz}), and $7b_1$ (d_{xz}) orbitals of the Pt_6 cluster (Model II).

Figure 9. SCF-Xα-SW molecular-orbital energy levels for $Pt(PH_3)_4$. Levels are labeled according to the irreducible representations of the C_{2v} point group. (PH_3) 1

Figure 10. Contour maps for the $8a_1$ (d_{z^2}, HOMO) and $5b_2$ (d_{yz}) levels of $Pt(PH_3)_4$.

Figure 11. SCF-Xα-SW molecular-orbital energy levels with relativistic corrections for the ten-atom cluster representation of the unreconstructed Pt(100) surface.

Figure 12. SCF-Xα-SW molecular-orbital energy levels with relativistic corrections for $Pt(PH_3)_4$.

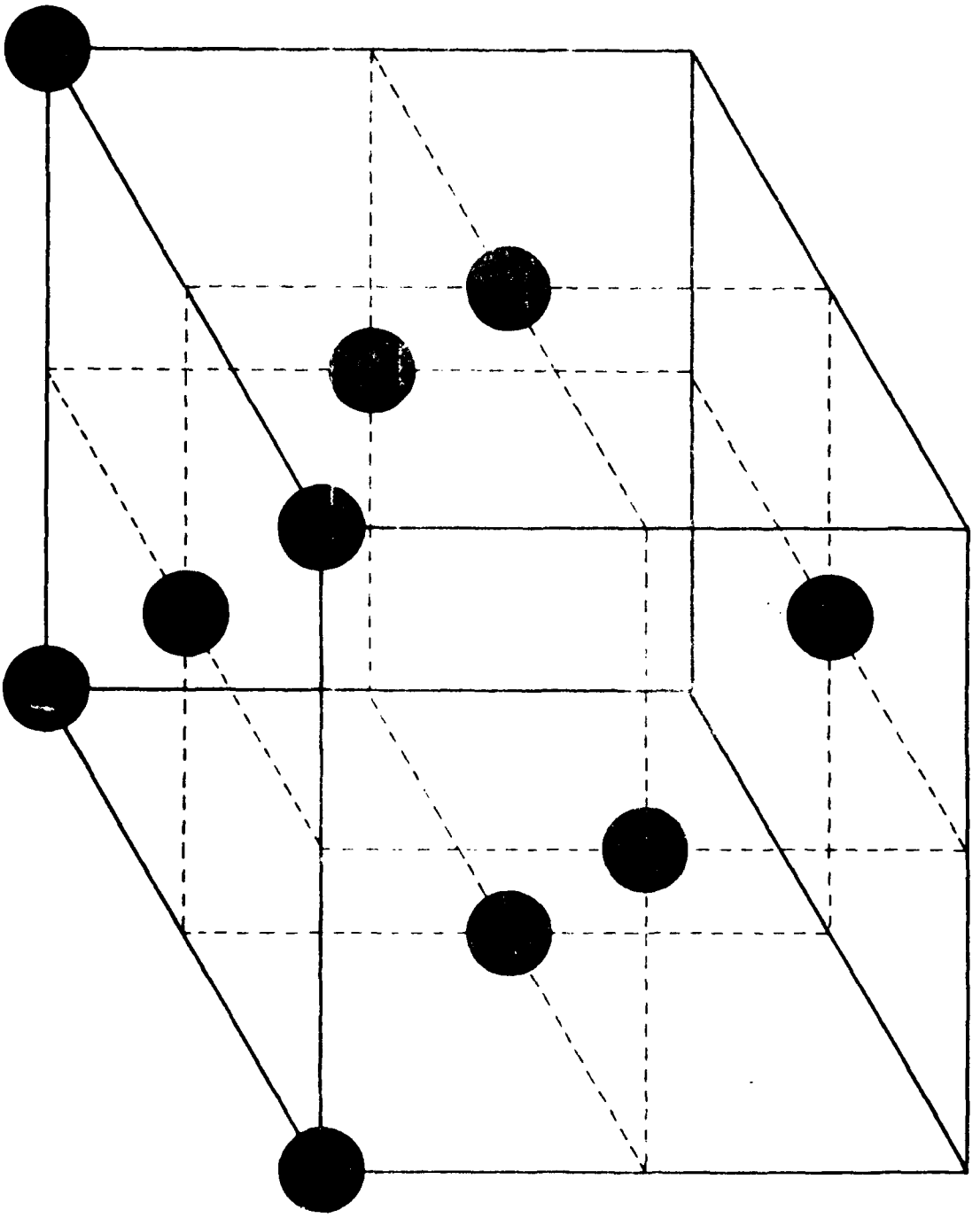

Figure 1

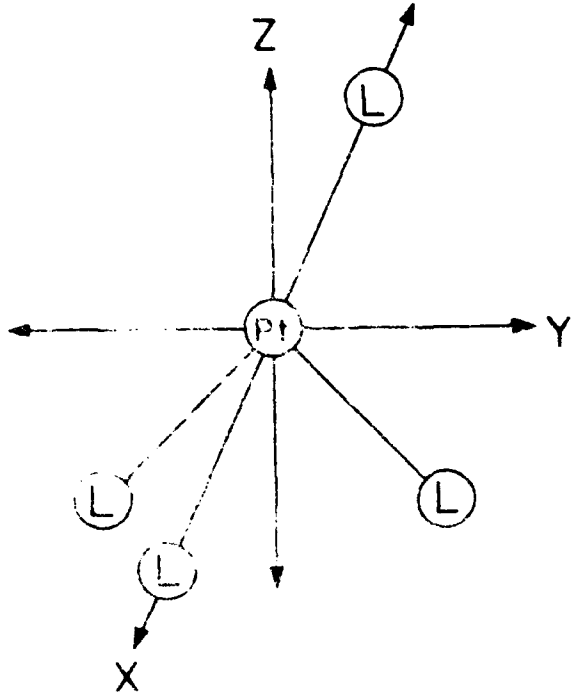

L= Pt, PH_3

MODEL I

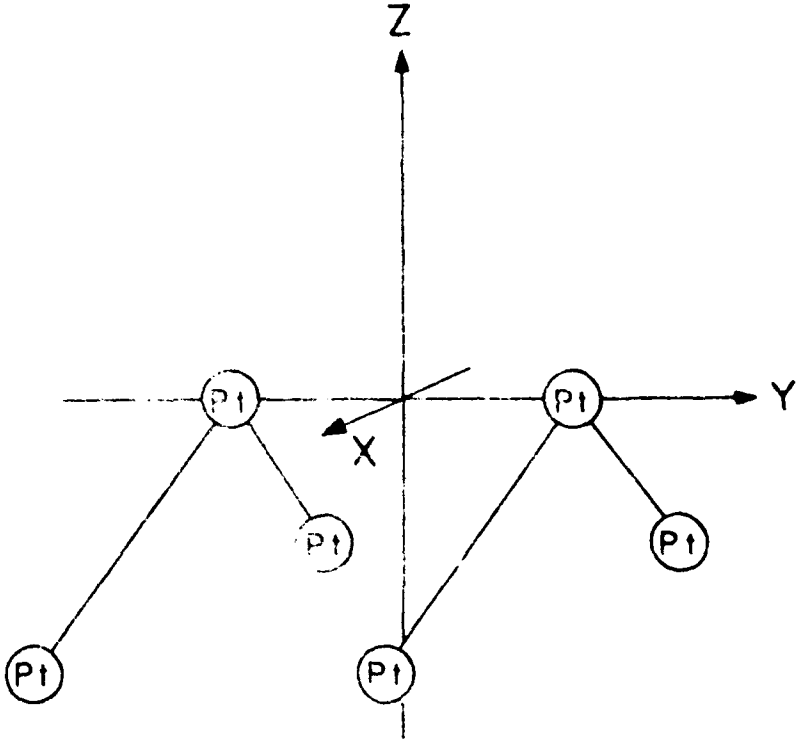

MODEL II

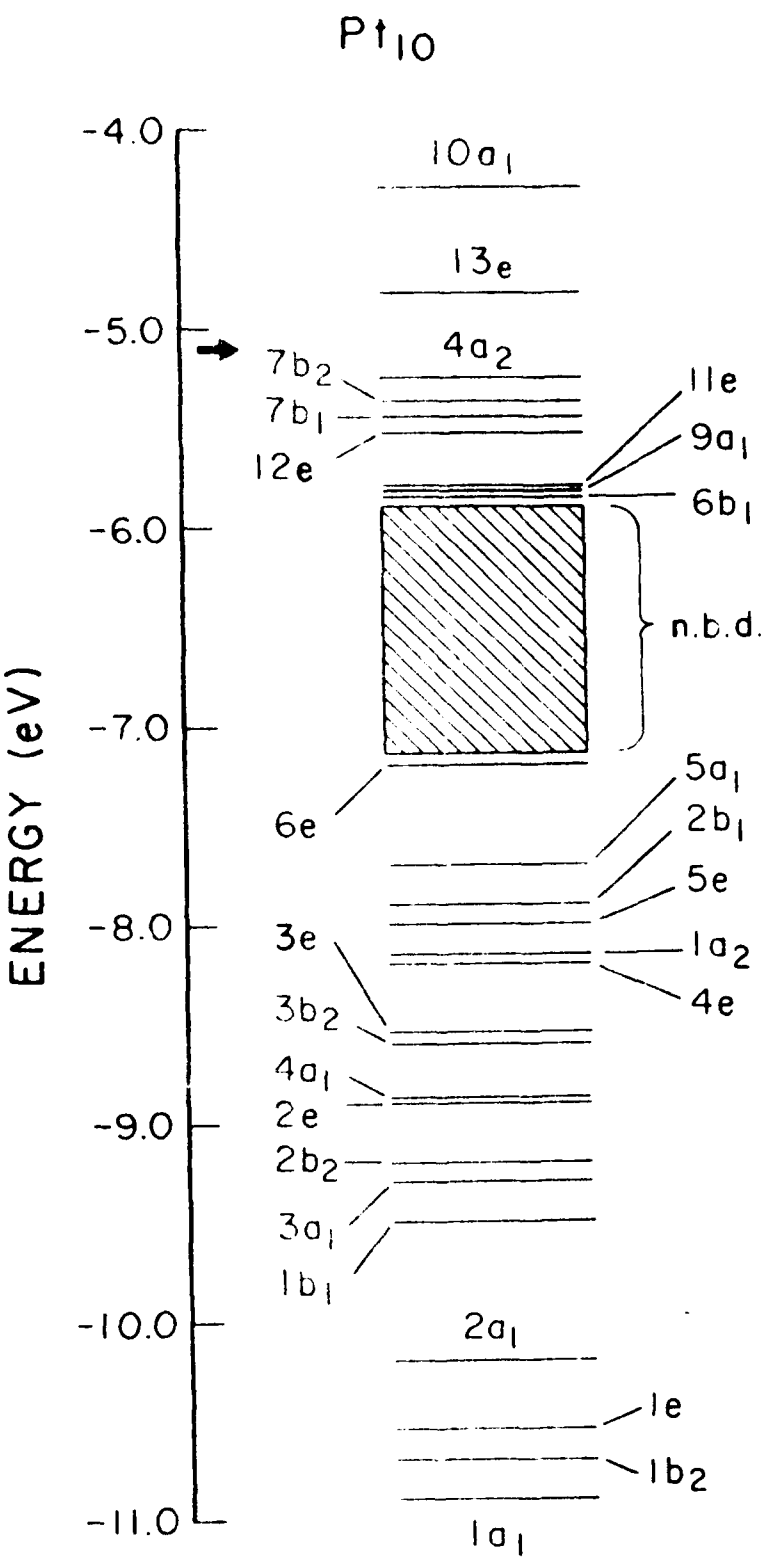
Pt10
ENERGY (eV)
-4.0
-5.0
-6.0
-7.0
-8.0
-9.0
-10.0
-11.0
10a1
13e
4a2
7b2
7b1
12e
11e
9a1
6b1
n.b.d.
6e
5a1
2b1
5e
1a2
4e
3e
3b2
4a1
2e
2b2
3a1
1b1
2a1
1e
1b2
1a1

Figure 3

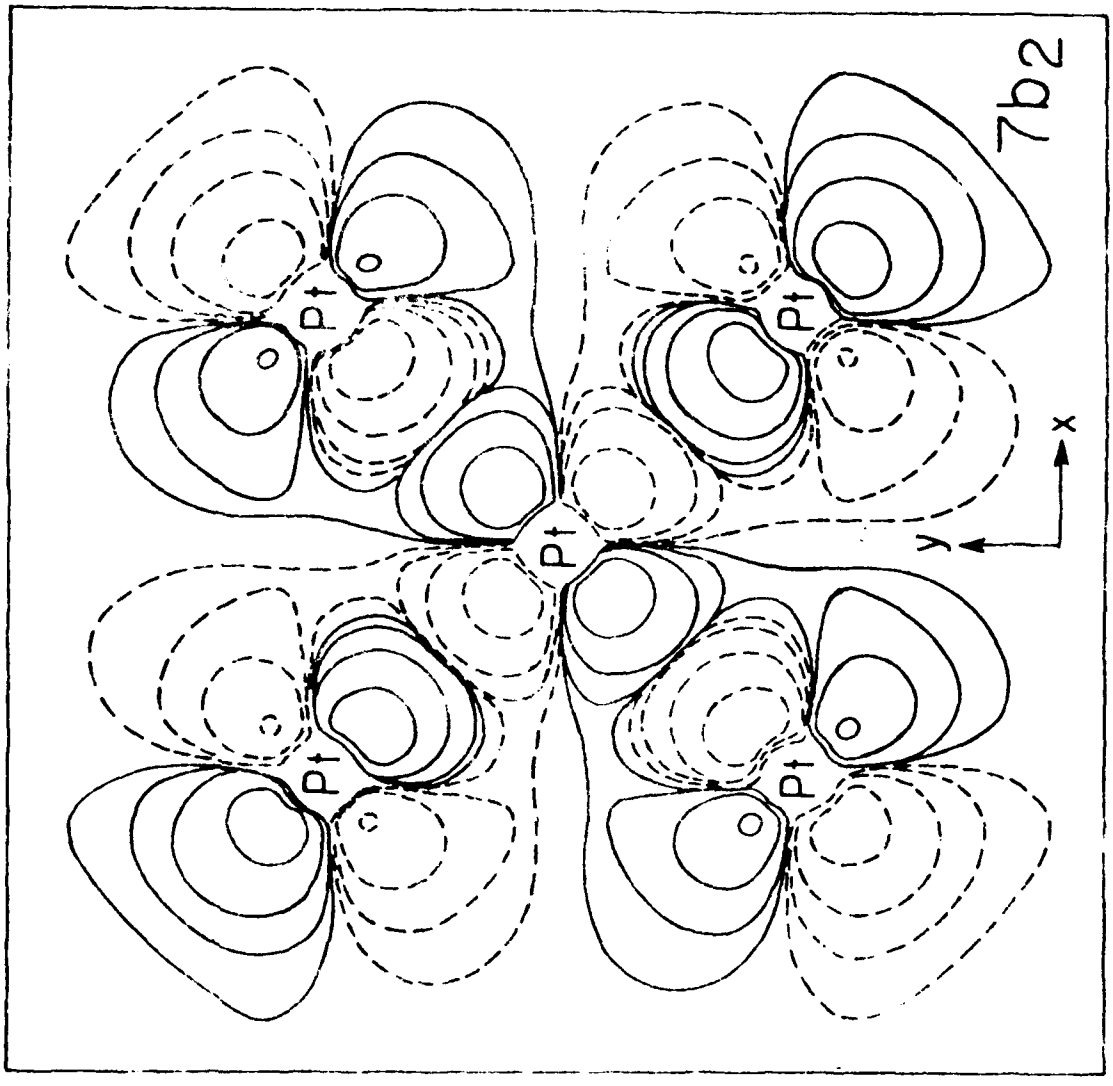

Figure 4

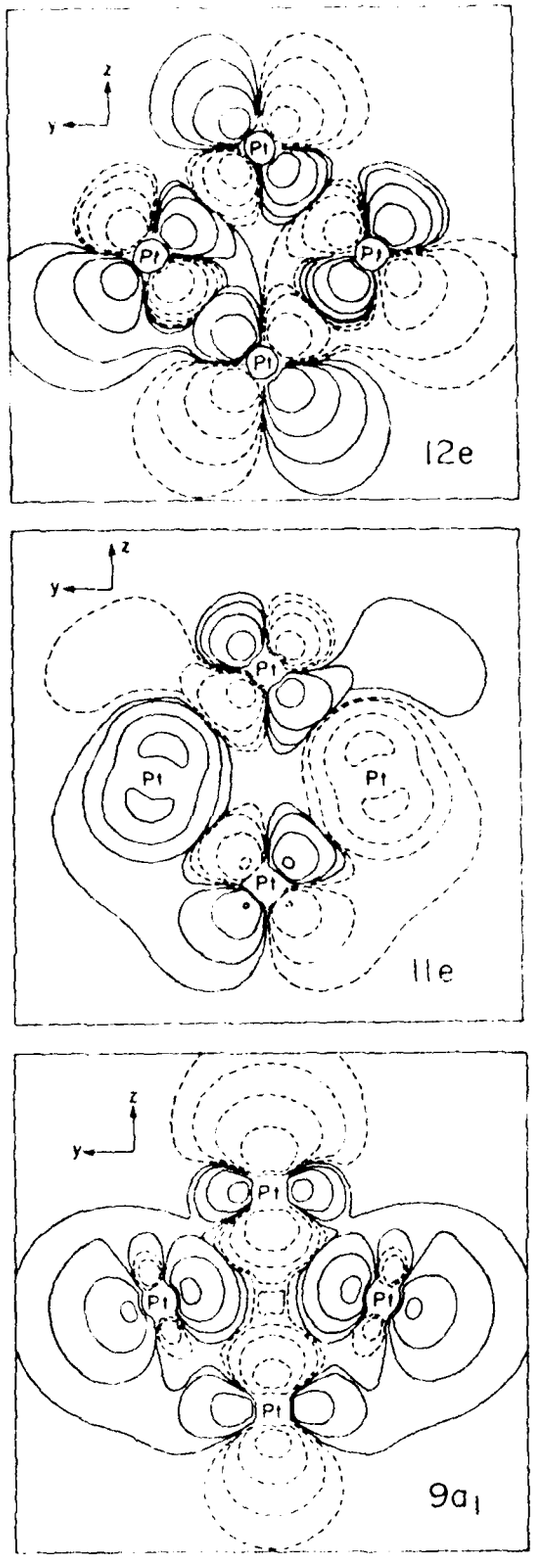

Figure 5

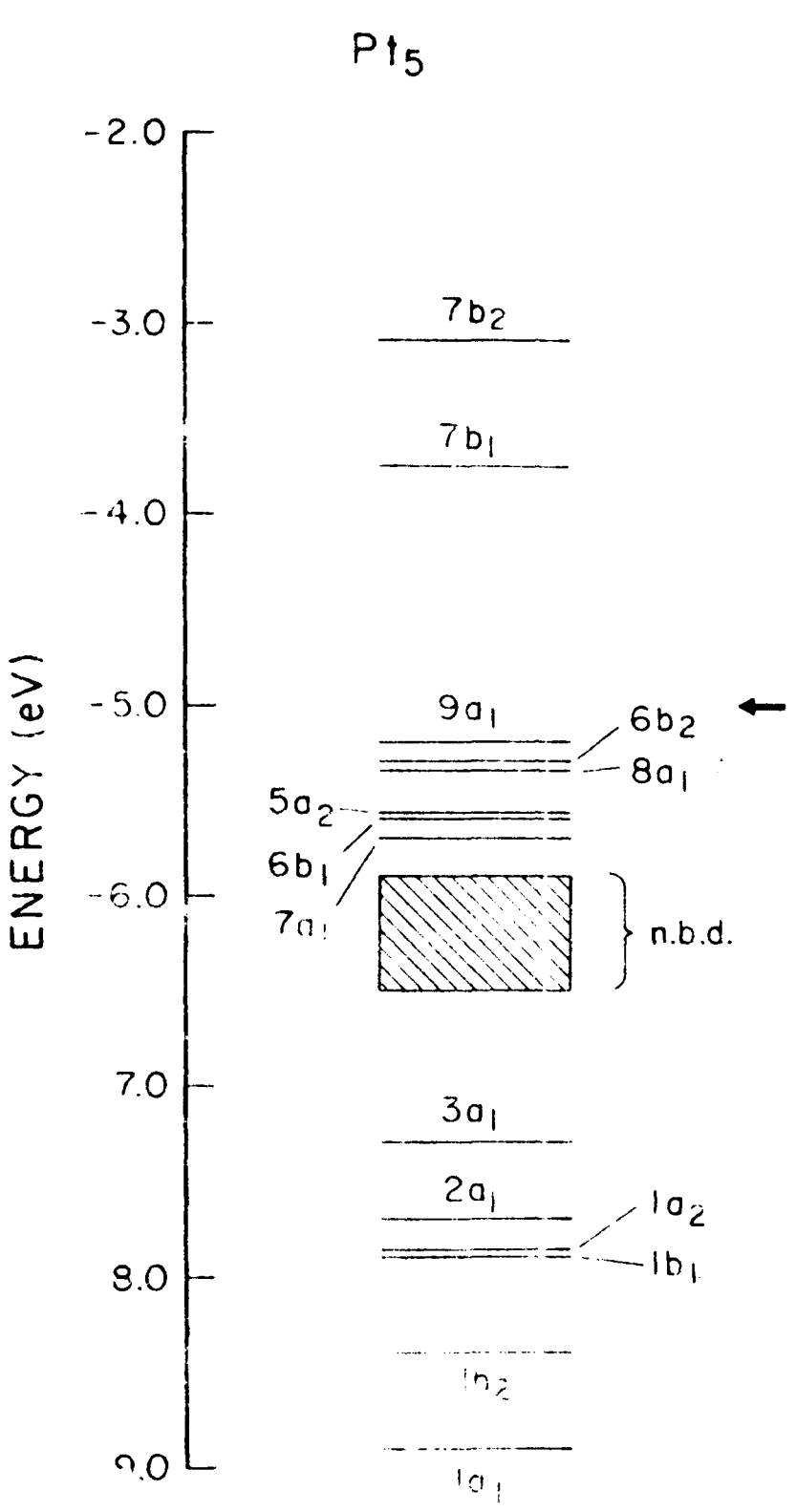
Pt5
-2.0
-3.0
-4.0
-5.0
-6.0
7.0
8.0
9.0
ENERGY (eV)
7b2
7b1
9a1
6b2
8a1
5a2
6b1
7a1
n.b.d.
3a1
2a1
1a2
1b1
1b2
1a1

Figure 6

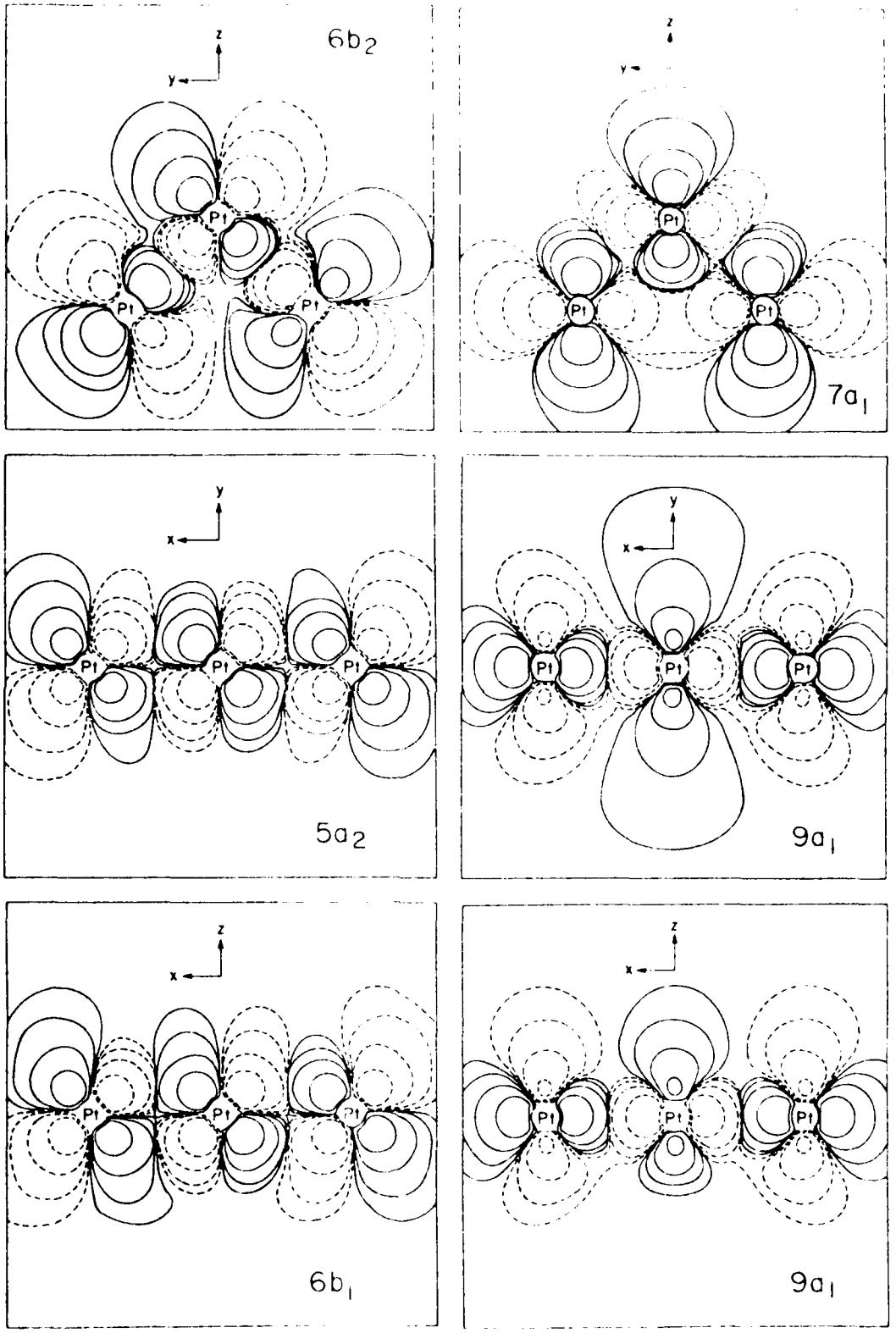
6b2
z
y
Pt
Pt
Pt
7a1
z
y
Pt
Pt
Pt
y
x
Pt
Pt
Pt
5a2
y
x
Pt
Pt
Pt
9a1
z
x
Pt
Pt
Pt
6b1
z
x
Pt
Pt
Pt
9a1

Figure 7

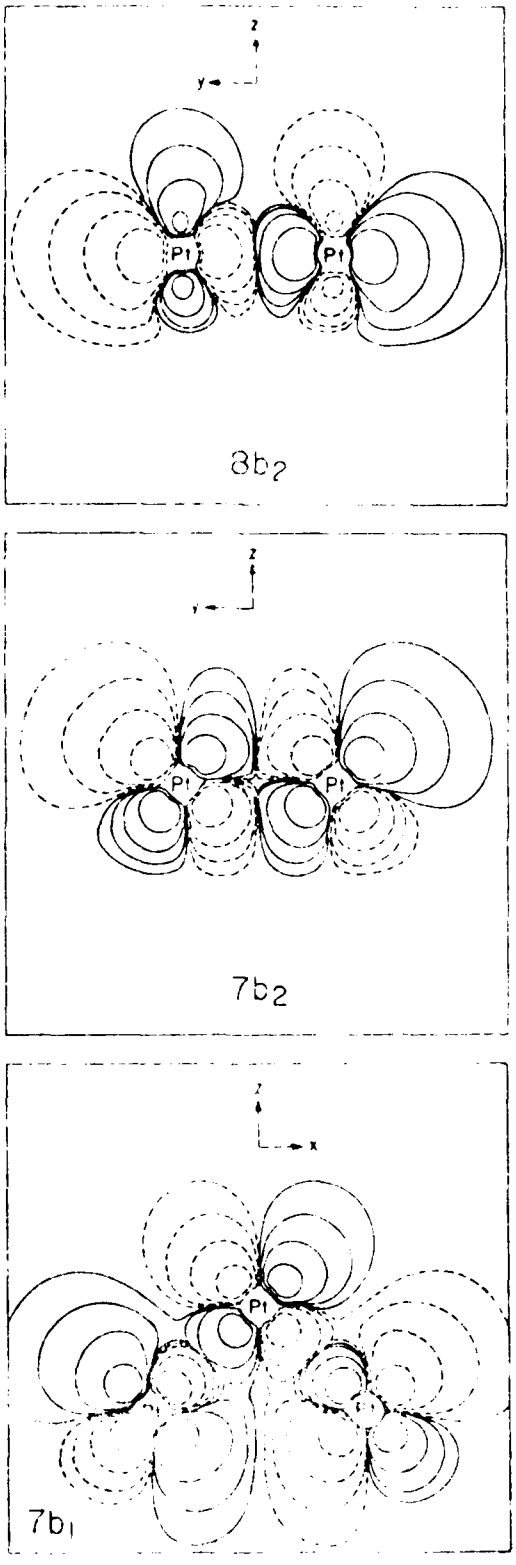

Figure 8

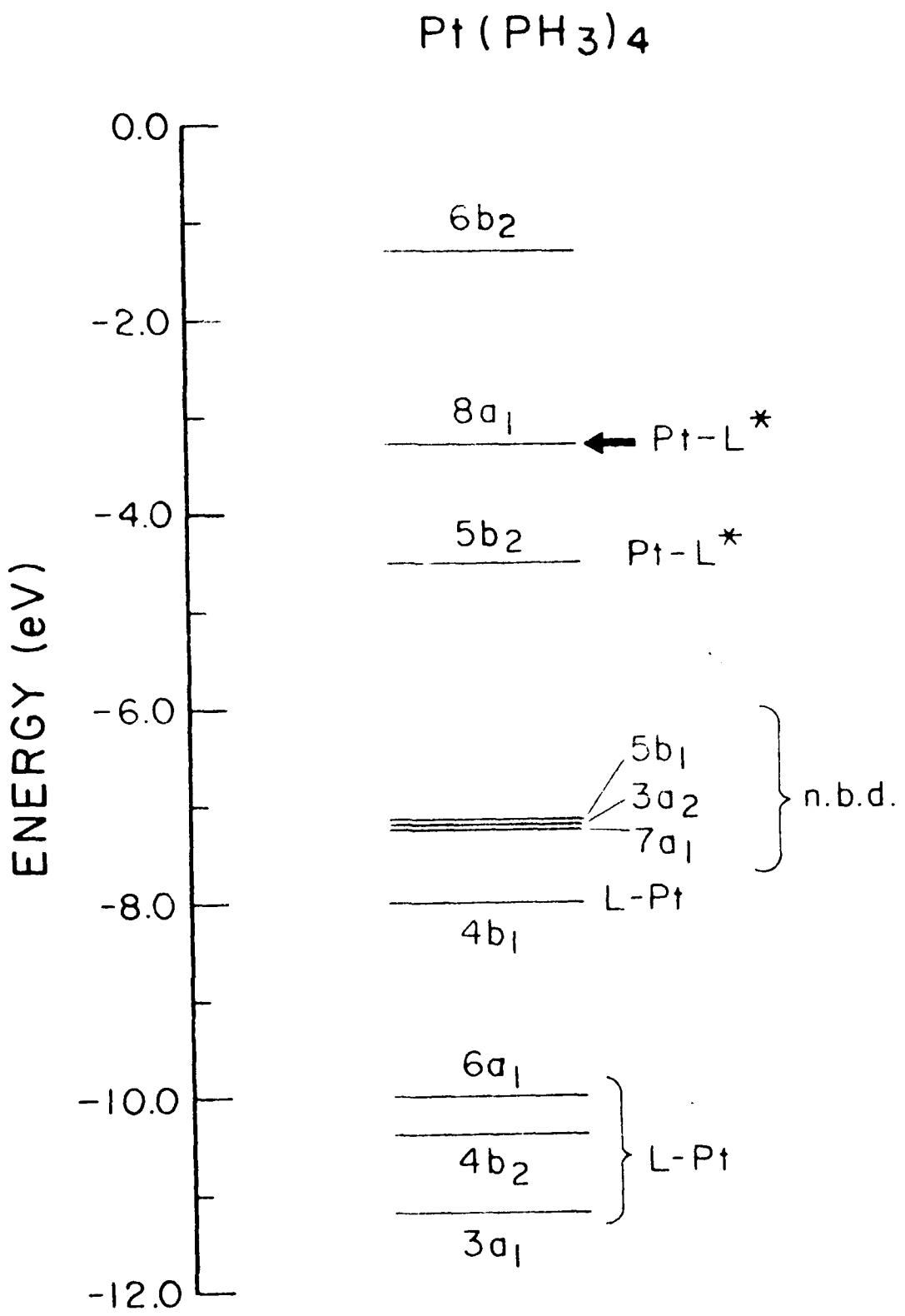
Pt(PH3)4
ENERGY (eV)
0.0
-2.0
-4.0
-6.0
-8.0
-10.0
-12.0
6b2
8a1
Pt-L*
5b2
Pt-L*
5b1
3a2
7a1
n.b.d.
L-Pt
4b1
6a1
4b2
3a1
L-Pt

Figure 9

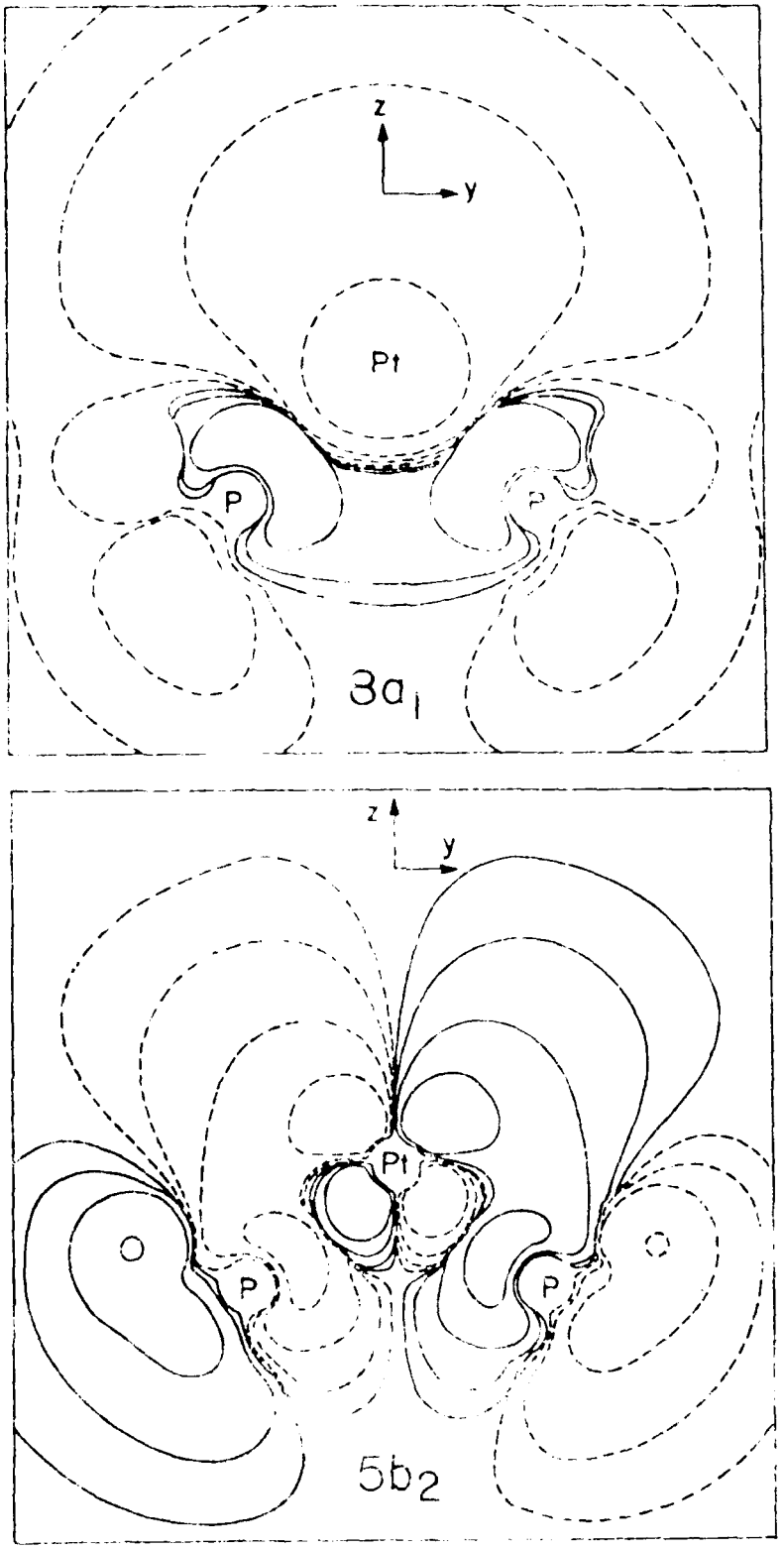

Figure 10

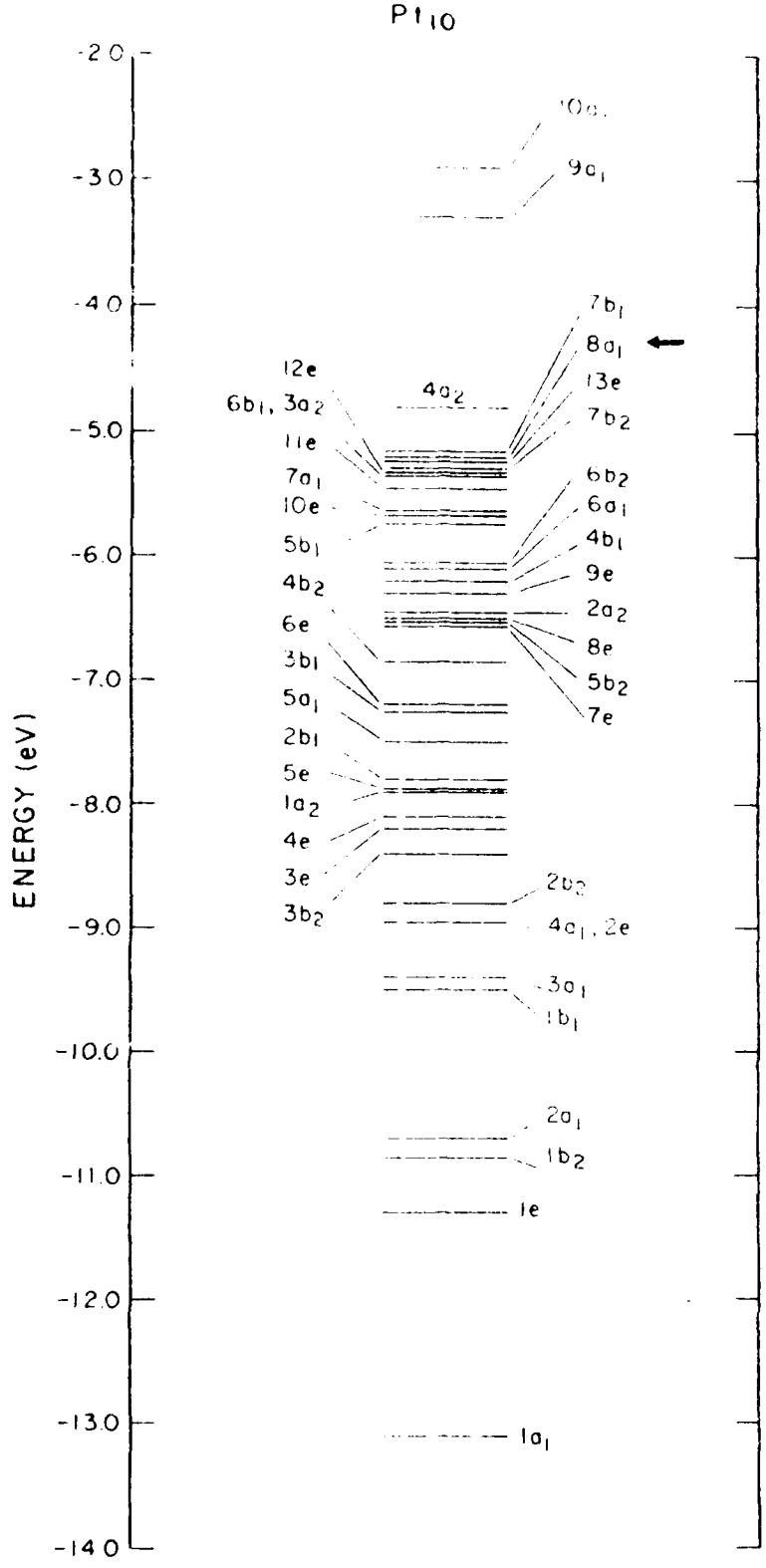
Pt10
ENERGY (eV)
-2.0
-3.0
-4.0
-5.0
-6.0
-7.0
-8.0
-9.0
-10.0
-11.0
-12.0
-13.0
-14.0
10a1
9a1
7b1
8a1
12e
6b1, 3a2
4a2
13e
7b2
11e
7a1
6b2
10e
6a1
5b1
4b1
4b2
9e
2a2
6e
8e
3b1
5b2
5a1
7e
2b1
5e
1a2
4e
3e
2b2
3b2
4a1, 2e
3a1
1b1
2a1
1b2
1e
1a1

Figure 11

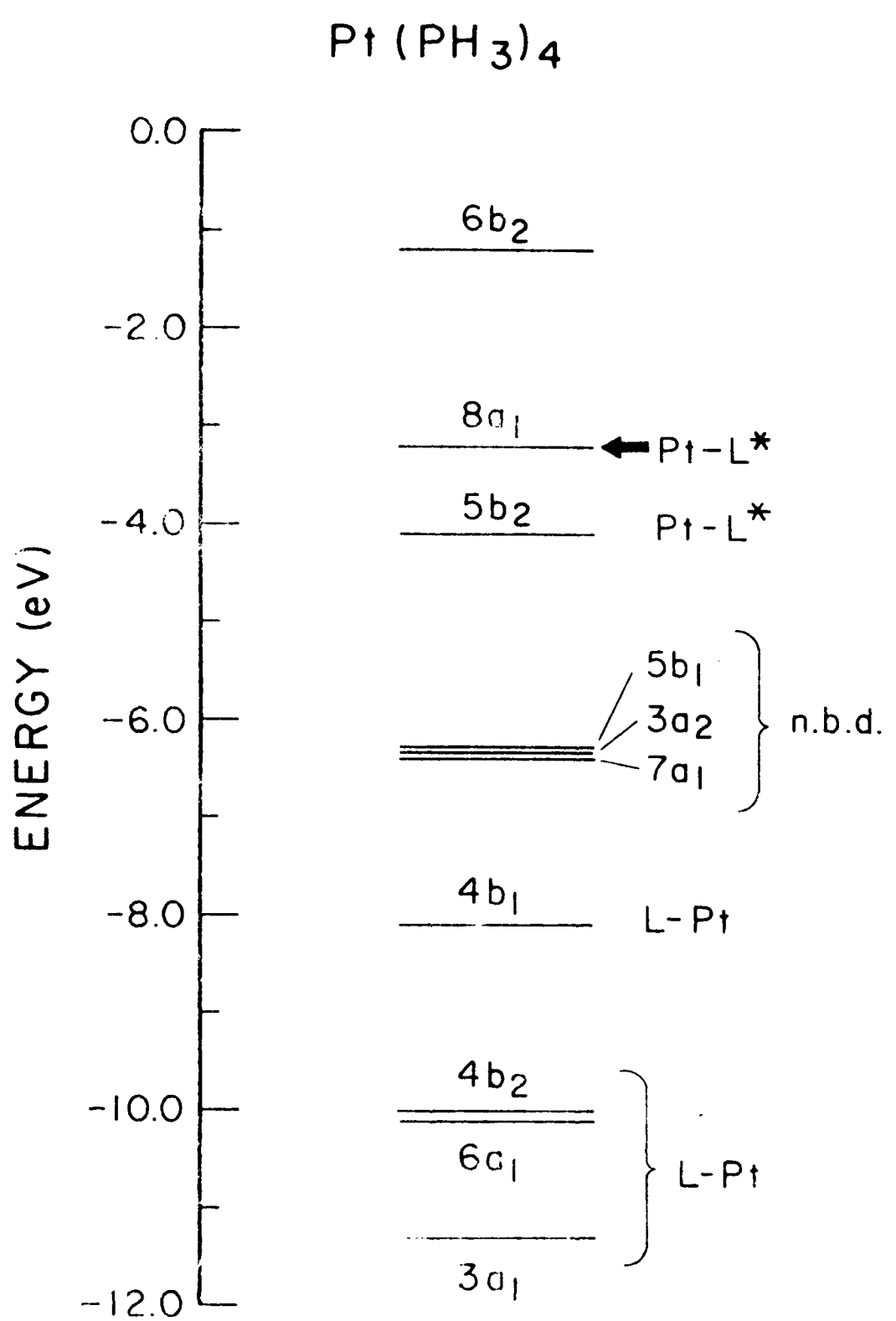
Pt(PH3)4
0.0
-2.0
-4.0
-6.0
-8.0
-10.0
-12.0
ENERGY (eV)
6b2
8a1
Pt-L*
5b2
Pt-L*
5b1
3a2
7a1
n.b.d.
4b1
L-Pt
4b2
6a1
3a1
L-Pt

Figure 12

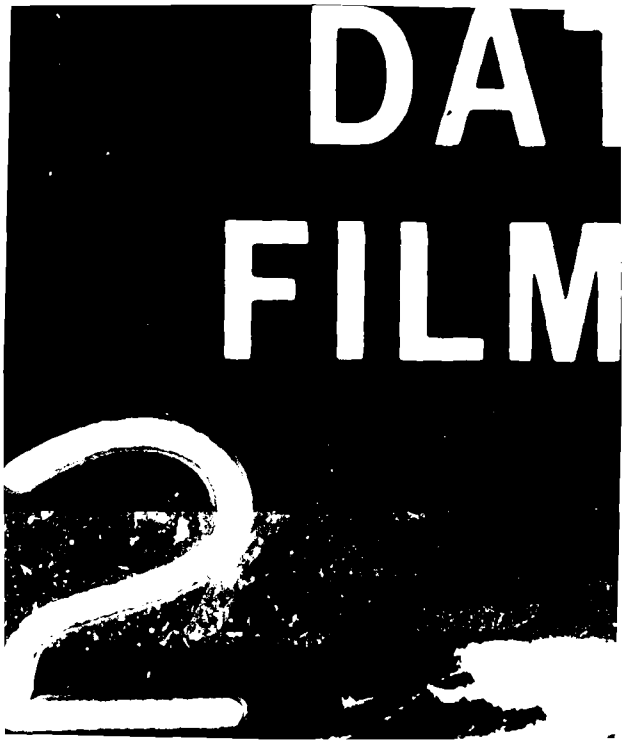
DA
FILM